NATIONAL AERONAUTICS AND SPACE ADMINISTRATION

Technical Report No. 32-741

Design Study of a Fission-Electric Cell Reactor

Jerome L. Shapiro

JET PROPULSION LABORATORY
CALIFORNIA INSTITUTE OF TECHNOLOGY
PASADENA, CALIFORNIA

August 1, 1965

NATIONAL AERONAUTICS AND SPACE ADMINISTRATION

Technical Report No. 32-741

Design Study of a Fission-Electric Cell Reactor

Jerome L. Shapiro

R. J. Mackin, Jr., Manager
Physics Section

JET PROPULSION LABORATORY
CALIFORNIA INSTITUTE OF TECHNOLOGY
PASADENA, CALIFORNIA

August 1, 1965

CONTENTS

TABLES

TABLES (Cont'd)

FIGURES

ABSTRACT

32198

A design approach is developed for the application of a fission–electric cell reactor to the generation of power in space. For a graphite-moderated reactor, the total size, temperature, and total (thermal) power are fixed. The remaining parameters, including cell dimensions and voltage, are then selected to optimize the overall efficiency. To simplify the calculations, two-group reactor theory is used, investigating both the single-region and two-region core concepts.

From the standpoint of overall efficiency, it is shown that the two-region core is advantageous only for low-efficiency systems and hence offers little promise. Another important result of these calculations is that the optimum operating voltage is shifted downward from the optimum as calculated without considering criticality limitations. This means that the maximum efficiency achievable is reduced considerably and indicates that the criticality requirement may be a more severe limitation on efficiency than the effect of voltage breakdown within the cell.

I. INTRODUCTION

The fission–electric cell reactor concept involves the direct utilization of the energy of fission fragments by allowing those charged particles to do work against an electrostatic potential (Ref. 1). An important limitation to its feasibility is the energy loss (in the form of heat) of the fragments within the fuel layer. Analyses of the efficiency obtainable indicate that reasonably high efficiency can result for very thin fuel layers (Ref. 2).

It may be observed that by choosing a small enough fuel thickness the efficiency can be made as high as fragment physics permits. The problem of reactor criticality would then be solved (for stationary power applications) by simply making the reactor big enough. While this approach may be adequate in some applications, it is clearly not so for a space-power plant. If a useful space-power plant is to be designed it must satisfy size and

weight restrictions. It may therefore be more logical in that case to begin with a certain fixed size limitation. From this, a critical mass limitation is inferred, which may then be translated into a limitation on minimum fuel thickness. The result may be that the achievable efficiency for that particular size of reactor is considerably less than the fragment-escape calculation alone would dictate.

This Report describes such a procedure for estimating the highest efficiency obtainable, starting with a fixed size and total power rating. A particular moderator material (graphite) and an average operating temperature have also been assumed. Of course it would simplify the designer's problem considerably if these could also be included as parameters, but this would complicate the method severely.

Owing to the relatively complex nature of the interaction between variables, the physical analysis was kept as simple as possible. Although this casts some doubt on the exact numerical results, estimates of the possible error of each individual portion of the calculation permit analysis of the overall error. In practice the error associated with the critical mass estimate will probably overshadow the errors from all other sources.

The analytic technique can best be described by dividing it into three areas:

1. Neutronics

2. Fission-fragment physics

3. Voltage breakdown

In (1), the main concern is finding the fuel requirement (critical mass plus burnup) as a function of reactor density. In the case of the two-region concept (Ref. 3), the fuel distribution is an additional variable.

In (2), the efficiency associated with the collection of fission-fragment energy is examined for varying fuel-layer thickness, cell geometry (specifically, the ratio of anode to cathode radius), and cell voltage.

In (3), some estimates are presented of the limitation on electrode-gap distance due to the effects of voltage breakdown across the gap.

For a given choice of overall size, shape, materials, and operating temperature, the three effects discussed above can be combined, optimizing the variables to give the maximum overall efficiency.

II. NEUTRONICS

A. Criticality Calculations

Methods are given below for the calculation of neutron physics parameters for both single-region and two-region reactor concepts. The single-region concept refers, of course, to a simple, unreflected reactor with uniform fuel loading. In the two-region concept, fuel and moderator densities are different in the two core regions.

1. Single-Region Concept

Using the age formulation of the criticality condition (Ref. 4), one may find the required fuel cross section from

$$\sum_a^F = \frac{1 + (L^M)^2 B^2}{\eta \, e^{-B^2 \tau} - 1} \sum_a^M \quad cm^{-1}$$

and the critical mass from

$$m = \frac{A}{N_0 \, \sigma_f} V \sum_a^F \quad gm.$$

2. Two-Region Concept

The two-region concept, in which a central, compact, non-power-producing cylinder produces neutrons that escape to the outer fission cell annulus, has been discussed in a previous report (Ref. 3). It was shown there that under certain conditions the efficiency reduction due to the unused energy released in the central region could be overcome by the increase in efficiency in the outer region due to the reduction of fuel thickness.

An estimate can be made of the net effect by arbitrarily reducing, by a fraction X, the amount of fuel necessary for criticality (as calculated above). Then by the methods outlined previously (Ref. 3) the Efficiency Reduction Factor (ERF) can be calculated. In this fashion the reactor may be described as a two-region system which in the limit of $X \to 1$ (ERF = 1) becomes a single-region system. The following parameters are required as input to the calculation for the ERF, in addition to those given above:

$$k_\infty(X) = \eta \frac{X\left(\sum_a^F / \sum_a^M\right)}{1 + X\left(\sum_a^F / \sum_a^M\right)},$$

$$L^2(X) = \frac{(L^M)^2}{1 + X\left(\sum_a^F / \sum_a^M\right)}.$$

B. Input Information

Input information includes fixed parameters, nuclear constants, neutron streaming effects, and the burnup requirement.

1. Fixed Parameters

In order to keep to a minimum the time and expense involved in the calculation it was necessary to fix some of the parameters. Although this was done in a somewhat arbitrary manner, the parameters were chosen with space applications in mind. It is anticipated that the reactor core will be large and heavy; therefore, it must have a high power output to justify its use. Furthermore, a major advantage of this type of electrical power system in space would be the savings in radiator weight due to high-temperature heat rejection. With these points in mind, the following choices were made:

Reactor core dimensions (unreflected)	10 ft long × 10 ft in diameter
Thermal power level	500 Mw
Average core temperature	2000 °K
Moderator	Graphite
Fuel	U^{235}
Operating time between refuelings	30 days

2. Nuclear Constants

The basic nuclear constants used here are:

$$U^{235}$$

2200 m/sec	2000 °K
$\sigma_a = 684$ b	$\sigma_a = 211$ b
$\sigma_f = 582$ b	$\sigma_f = 174$ b
$\nu = 2.47$	$\eta = 2.04$

Graphite

293 °K	2000 °K
$\Sigma_a = 0.00026$ cm^{-1}	$\Sigma_a = 0.00009$ cm^{-1}
$L^2 = 2352$ cm^2	$L^2 = 6270$ cm^2
$\tau = 350$ cm^2	$\tau = 329$ cm^2

The uranium data at 2200 m/sec are the "World Consistent Set" (Ref. 5). The correction for temperature and "non-1/v" was taken from the *Reactor Physics Constants* handbook (Ref. 6). The latter was also the source of the graphite data. No correction for thermal expansion was made.

3. Neutron Streaming Effects

The reactor will be in the form of a graphite cylinder pierced by many annular holes. The annuli are formed by the vacuum space between the cylindrical cathode and anode of each cell. The critical mass formulae assume the core to be homogeneous. However, Behrens (Ref. 7) showed that the effect of lumped voids is to increase both the effective age and the diffusion length as calculated from homogenized data.

Applying Behrens' formulae directly (neglecting fuel absorption) the increase in the migration area due to the heterogeneity of the voids can be expressed in the form

$$(1-\alpha)^2 + \alpha(1-\alpha) \left\{ \left[\frac{t^2}{2D_c + t} \right] \right.$$

$$\left[\frac{3}{\exp\left[\frac{3t^2}{2D_c+t}\left(\frac{1-\alpha}{\alpha}\right) \right] - 1} + \frac{1.28}{1 + \frac{t}{D_c}} + 1.68 \right] + 2 \right\},$$

where

$D_c \equiv$ diameter of cathode,

$D_A \equiv$ diameter of anode,

$t \equiv D_A - D_c$.

Table 1. Neutron streaming correction factors

α	t, cm	D_c, cm	$\dfrac{M^2 \text{ (Behrens)}}{M^2 \text{ (Homogeneous)}}$
0.5	2	3	1.16
0.5	2	5	1.11
0.4	2	3	1.17
0.4	2	5	1.12

In this formula the neutron mean free path has been assumed to be 3 cm. Table 1 shows the resulting effects for several choices of void fraction and cathode diameter for an assumed gap of 1 cm. This effect is obviously a variable. However, because of the complexity of the calculation, the approximate nature of the results, and the relatively small variation found in Table 2, a constant value of 1.15 is used in this study. Thus the diffusion

Table 2. Variation of neutron parameters and critical mass with the void fraction

α	τ, cm²	$(L^M)^2$, cm²	Σ_a^M, cm⁻¹	Σ_a^F, cm⁻¹	m, kg	m', kg	B_z^2, cm⁻²
0.25	781	15653	0.0000675	0.0008081	33.3	48.3	1.86 × 10⁻⁴
0.35	1040	20840	0.0000585	0.001198	49.4	64.4	1.47
0.40	1220	24460	0.0000540	0.001624	67.0	82.0	1.32
0.45	1452	29107	0.0000495	0.002573	106.1	121.1	1.18

Table 3. Results of criticality calculations

X	k_∞	L^2	$\mathcal{M}$	ERF	$Xm'/\alpha V$
			α = 0.25		
1	1.929	852.6	∞	1	8.67
0.8	1.905	1052	6.82	0.872	6.94
0.6	1.862	1371	2.53	0.717	5.20
0.4	1.784	1970	1.13	0.531	3.47
0.2	1.584	3500	0.417	0.294	1.73
0.1	1.296	5720	0.189	0.159	0.87
			α = 0.35		
1	1.964	752.3	∞	1	8.25
0.8	1.945	932.0	6.91	0.874	6.60
0.6	1.918	1226	2.63	0.725	4.95
0.4	1.863	1882	1.11	0.526	3.30
0.2	1.717	3290	0.465	0.317	1.65
0.1	1.481	5680	0.203	0.169	0.83
			α = 0.40		
1	1.986	646.9	∞	1	9.19
0.8	1.975	805.0	6.97	0.875	7.35
0.6	1.950	1060	2.63	0.725	5.51
0.4	1.912	1560	1.24	0.554	3.68
0.2	1.797	2950	0.485	0.327	1.84
0.1	1.604	5230	0.215	0.177	0.92
			α = 0.45		
1	2.007	483.0	∞	1	12.07
0.8	1.997	660.0	6.98	0.875	8.45
0.6	1.983	795.0	2.73	0.732	7.24
0.4	1.957	1178	1.30	0.565	4.83
0.2	1.885	2265	0.541	0.351	2.41
0.1	1.745	4200	0.240	0.194	1.21

area and the age, as calculated from homogenized data, are simply multiplied by 1.15.

4. Burnup Requirement

Additional fuel must be added to compensate for burnup. For these calculations, 15 kg is added, which would permit about 15,000 Mw-days of thermal power. This amount was chosen to yield approximately 10–25 Mwe over a 30-day period.

Thus after the amount of fuel required for criticality (m) is calculated, an addition of 15 kg is made, to give the total fuel loading (m'). This then makes the reactor initially supercritical. For calculational purposes it was assumed that control rods would be inserted from one end to reduce reactivity. It is therefore necessary

in each case to adjust the axial buckling to make the reactor critical at the start (with $X = 1$).

C. Results

The results of the criticality calculations are given in Tables 2 and 3. Although the intermediate data are reported for completeness, the most important results for each value of α are the ERF and the "minimum fuel-layer thickness characteristic." The latter parameter is derived from the loaded fuel mass Xm'. It is assumed that the dimensions of the cell will be chosen to maximize the cathode surface area. This will be discussed more fully later. The result, however, is that the minimum layer thickness may be expressed as the product of a geometric function and $(Xm'/\alpha V)$. Therefore the values of $Xm'/\alpha V$, termed the "minimum fuel-layer thickness characteristic," are tabulated.

III. FISSION-FRAGMENT PHYSICS

A. Model

Previous calculations (Ref. 2) of the efficiency of the fission–electric cell have employed a model assuming monoenergetic fission fragments. It was also assumed that a fragment's electric charge remained constant as the fragment passed through the fuel layer. These assumptions have been modified as follows:

Each fission is assumed to release one light and one heavy fragment. The light fragment has an initial charge number $Z_\ell^0 = 21$ and initial energy $E_\ell^0 = 100$ Mev. Values for the heavy fragment are $Z_h^0 = 23$ and $E_h^0 = 67$ Mev. Furthermore it is assumed that the charge on the light fragment varies as the square root of the velocity, while that of the heavy fragment varies as the velocity itself. Although there is little information concerning the ranges in solids for each fragment, on the basis of measurements reported in gases (Ref. 5) it will be assumed that the ranges are proportional to the initial energy.

Finally, the linear energy loss model originally used has been replaced with the assumption that the fission fragment velocity decreases linearly with penetration. Thus the equations presently being used for calculating

efficiency become (compare with Ref. 2, p. 21), for the cylindrical case:

$$\mathscr{E}_{\text{cell}} = \frac{E^0}{e} \frac{P}{\pi T}$$

$$\times \int_0^{\delta_{\text{max}}} d\delta \int_0^{\phi_{\text{max}}} d\phi \int_0^{r_{\text{max}}} (1 - r)^c \cos^2\phi \cos\delta \, dr,$$

where r_{max} is the smaller of

$$\begin{cases} 1 - \left[\dfrac{P}{\cos^2\phi \left(1 - \dfrac{R_1^2}{R_2^2} \sin^2\delta\right)} \right]^d, \\[4ex] \dfrac{\tau}{\cos\phi \cos\delta} \end{cases}$$

$$\cos^2\phi_{\text{max}} = \frac{P}{1 - \dfrac{R_1^2}{R_2^2} \sin^2\delta},$$

$$\sin^2\delta_{\text{max}} \text{ is the smaller of } \begin{cases} \dfrac{R_2^2}{R_1^2}(1 - P), \\[2ex] 1 \end{cases}$$
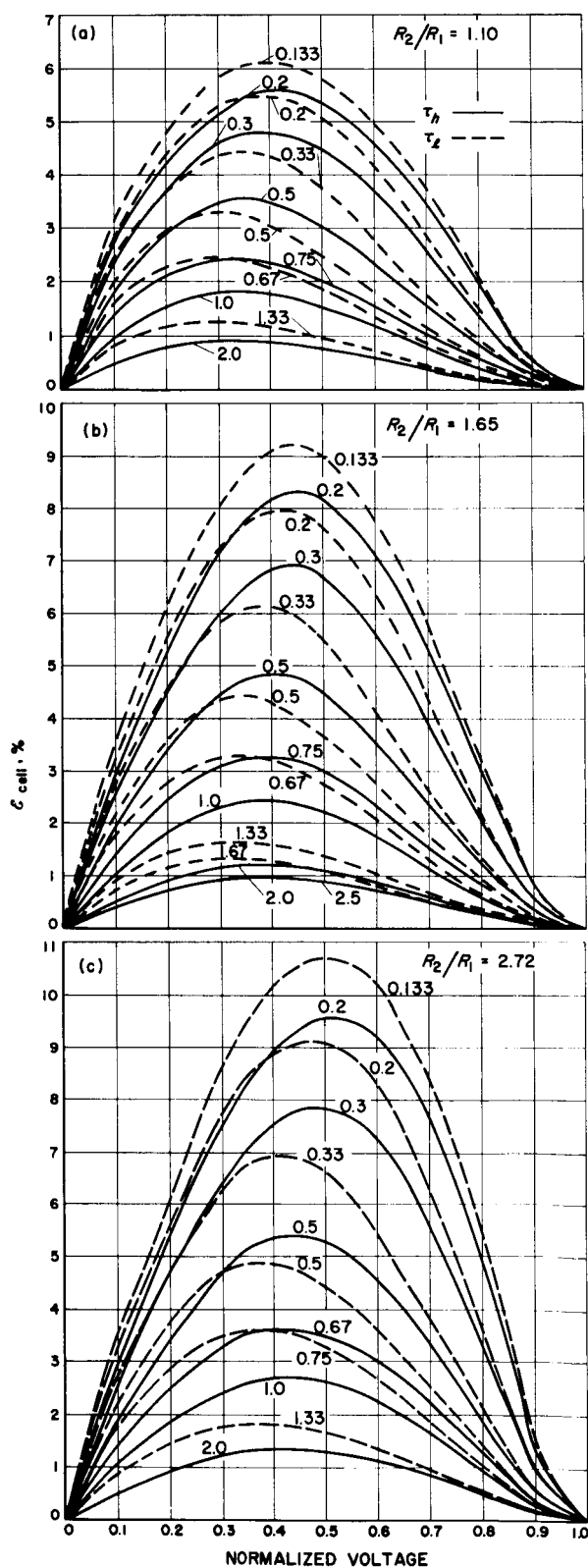
Fig. 1. Efficiency vs normalized voltage for cylindrical
electrode fission cell (numbers on the curves refer
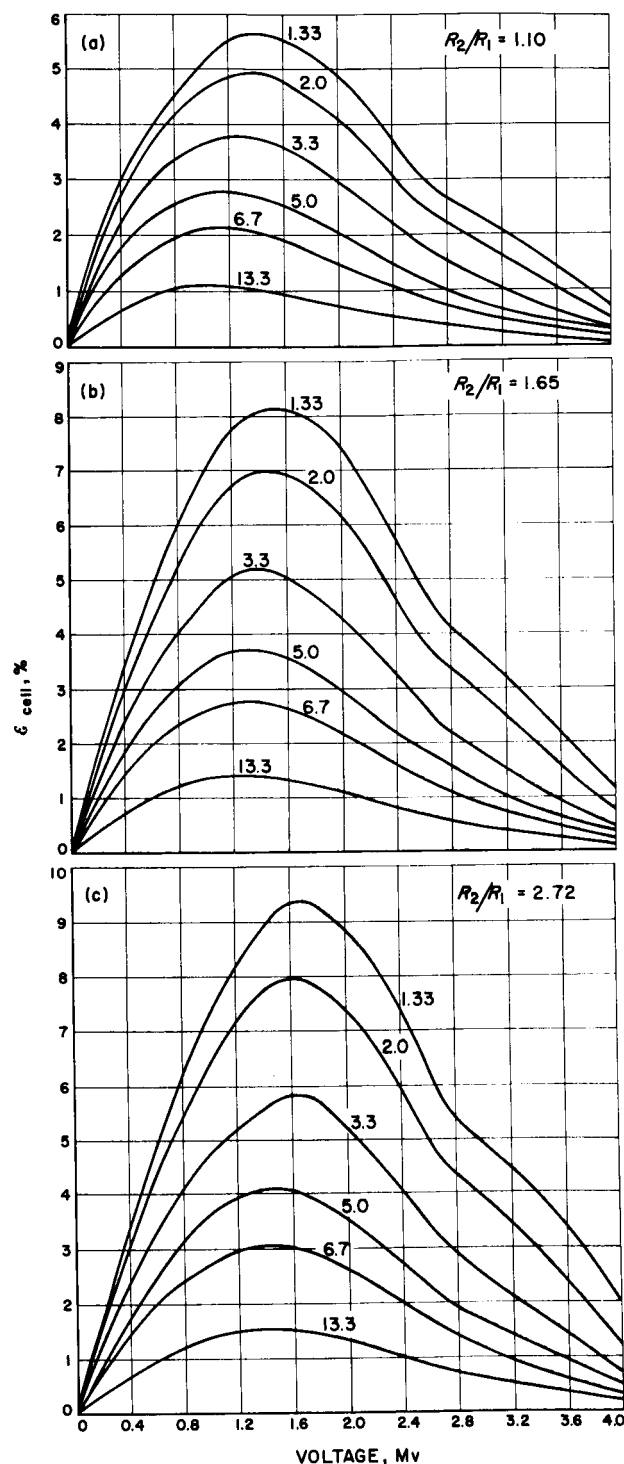to fuel-layer thickness in range units)

Fig. 2. Efficiency vs actual voltage for cylindrical
electrode fission cell (numbers on the curves
refer to the fuel-layer thickness in
mg/cm^2 of U$_3$O$_8$)

and $c = d = 1$, for the heavy fragment, while $c = 1/2$, $d = 2/3$, for the light fragment.

In these equations the voltage P is in units of E^0/e, where E^0 is initial fragment energy and e is initial fragment charge. Similarly, the fuel-layer thickness T is in units of fragment range. Therefore, for a given operating voltage and fuel thickness, separate calculations were made for the light and heavy fragments, and the results were combined to yield the actual efficiency.

B. Results

Figure 1 shows the resulting efficiency curves for various thicknesses, measured in units of maximum range of the particles, and for three ratios of anode to cathode radius. For any given thickness of material the efficiency is found from the average of the efficiencies of the light and heavy particle curves corresponding to that thickness. Table 4 shows the relationship between the thickness in range units, used in Fig. 1, and the thickness in terms of mg/cm^2 of U_3O_8. In combining curves it must be remembered that for any given potential differences between electrodes the normalized voltage will be different for the light and heavy fragments, owing to the difference in initial charge and energy. Table 5 shows the relationship between actual and normalized voltages.

With the aid of these tables, the curves of Fig. 1 were combined to form Fig. 2. These results were then replotted, as shown in Fig. 3, to permit interpolation of thicknesses for fixed voltages.

Table 4. Comparison of fuel-layer thickness units

Fragment type	Thickness, in range units, for indicated thickness of U_3O_8					
	1.33 mg/cm^2	2.0 mg/cm^2	3.3 mg/cm^2	5.0 mg/cm^2	6.7 mg/cm^2	13.3 mg/cm^2
Light	0.133	0.20	0.33	0.50	0.67	1.33
Heavy	0.20	0.30	0.50	0.75	1.0	2.0

Table 5. Comparison of normalized and actual voltages

Fragment type	Normalized voltage for indicated actual voltage										
	0	0.4 Mv	0.8 Mv	1.2 Mv	1.6 Mv	2.0 Mv	2.4 Mv	2.8 Mv	3.2 Mv	3.6 Mv	4.0 Mv
Light	0	0.084	0.168	0.252	0.336	0.420	0.504	0.588	0.072	0.756	0.840
Heavy	0	0.137	0.274	0.411	0.548	0.685	0.822	0.959	1.096	1.233	1.370
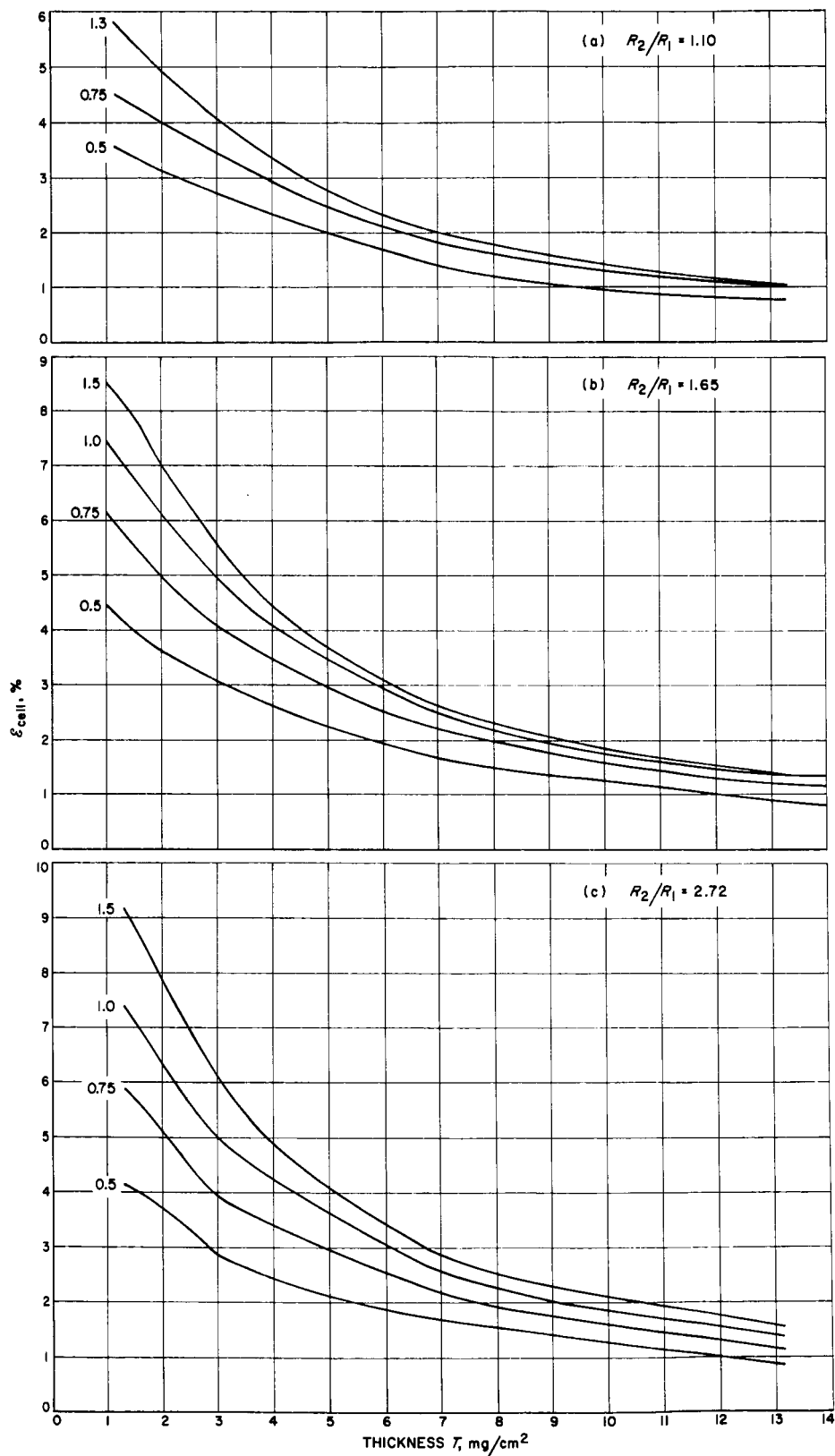
Fig. 3. Efficiency vs thickness for cylindrical electrode fission cell (numbers on the curves refer to actual voltage in megavolts)

IV. VOLTAGE BREAKDOWN

The phenomenon of voltage breakdown across a vacuum gap is not yet well understood. The subject has been attacked by many in recent years, without very good agreement. In the fission–electric cell reactor application the situation is even more in doubt, because it is difficult to predict the vacuum that will exist between anode and cathode.

With all the uncertainties involved, all that can be done at this stage is to estimate an upper and lower bound on the voltage breakdown point. This was done using the review report of Alpert and Lee (Ref. 8). The upper curve shown in Fig. 4 is an extrapolation of the linear effect found experimentally for small gaps (10^{-3} cm). This limit has not been achieved thus far across larger
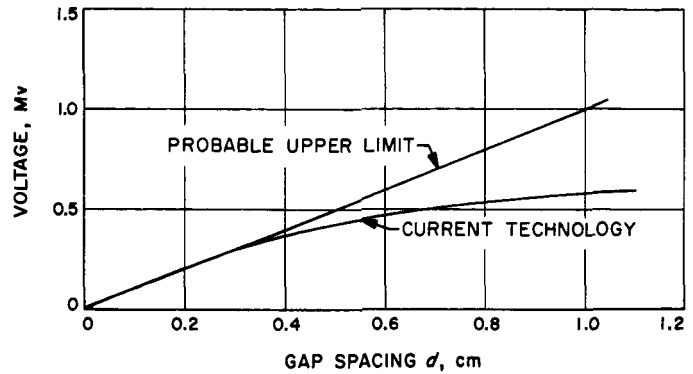
Fig. 4. Voltage breakdown in vacuum

gaps, but the curve is used as an upper bound. The lower curve represents presently achieved wide-gap voltages.

V. OPTIMIZATION

From the reactor physics calculations, with V fixed and with α and X as parameters, the required fuel mass Xm' and the ERF were determined. The fuel thickness is then simply Xm' divided by the fuel area S, which is a function of α, V, R_0, R_1 and R_2 (see Fig. 5).

The expression for minimum fuel thickness (derived in Appendix A) is

$$T = \frac{Xm'}{S} = \frac{Xm}{\alpha V}\left[\frac{d(1 + R_2/R_1) + \dfrac{R_0^2}{R_1}}{2}\right],$$

where

$$d = R_2 - R_1 \text{ (gap spacing)}.$$

At the risk of giving a slightly optimistic efficiency (by underestimating T) we set $R_0 = 0$. This leaves one parameter, d, which can be varied to show how T varies.

For each value of T, R_2/R_1, and voltage P, a cell efficiency $\mathcal{E}_{cell}$ was found from Fig. 3. Then the overall efficiency $\mathcal{E}$, the product of $\mathcal{E}_{cell}$ and ERF, was tabulated (these tables are included as Appendix B). For
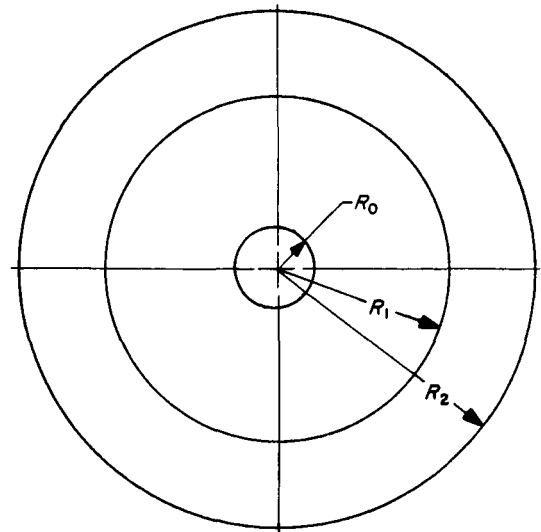
R_0 COOLANT CHANNEL RADIUS
R_1 CATHODE OUTER RADIUS
R_2 ANODE RADIUS

Fig. 5. Typical cell geometry

each value of d, R_2/R_1, and P, the highest efficiency was selected and plotted in Fig. 6 as a curve of constant $\mathcal{E}_{max}$ (dotted lines). Plots of the same information, with the restriction that $X = 1$, are also included (solid lines).

These iso-efficiency curves, together with the voltage breakdown limiting curves, which are superimposed on Fig. 6 as dashed lines, can be used to find the optimum operating point.
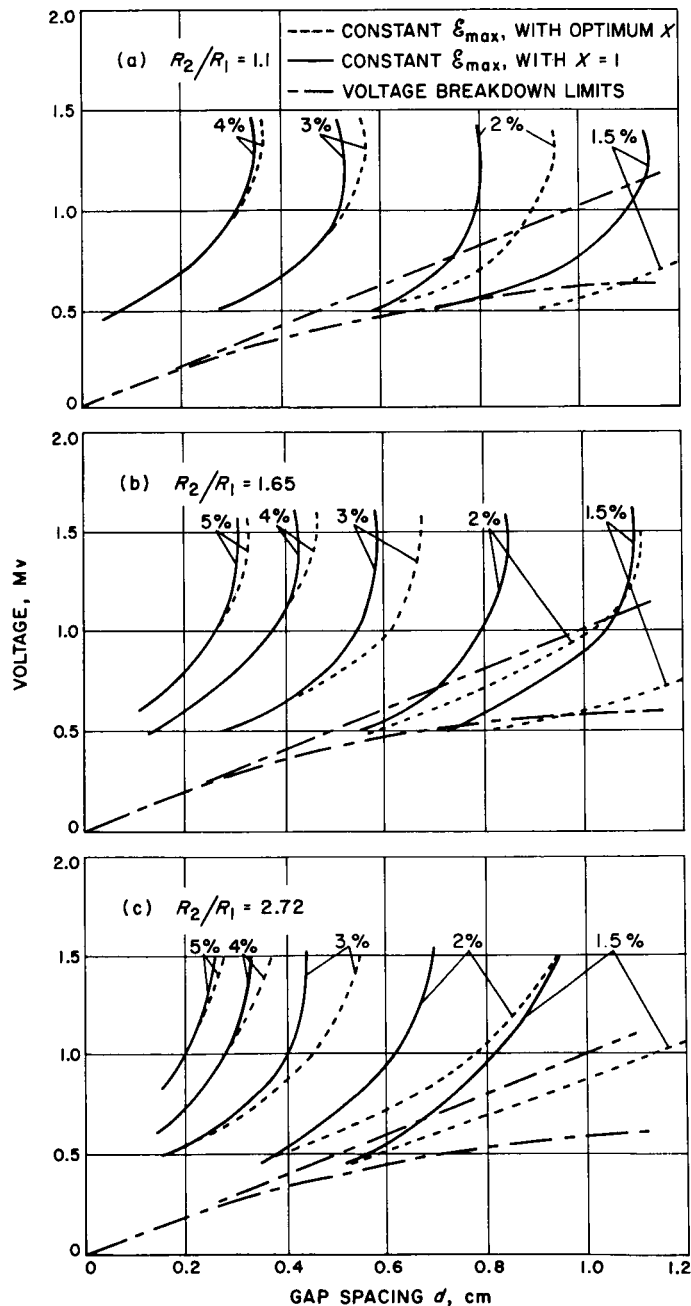
Fig. 6. Iso-efficiency curves

VI. DISCUSSION OF RESULTS

The curves of Fig. 6 represent the most important results of this work. Although the actual numbers are approximate since they are based on a very simple nuclear model, some important conclusions can be drawn from them.

As indicated previously, if R_0^2/R_1 is negligibly small, the fuel-layer thickness is directly proportional to the product dm'. The efficiency is, of course, dependent upon this thickness T. Therefore, a reduction in fuel loading m' may be exactly balanced by an increase in d. If the fuel requirements as calculated here could be cut by a factor of 2, then the same iso-efficiency curves could be used simply by dividing the d scale by the same factor. For example, we see on the curve of Fig. 6b $(R_2/R_1 = 1.65)$ that the maximum efficiency obtainable, taking the optimistic voltage breakdown curve, is slightly better than 2% (at a voltage of about 500 kv). If the fuel mass could be cut in half by refining the calculations or by conserving neutrons with the addition of a reflector, the efficiency could be increased to about 3.5% (at 650 kv).

By comparing the curves for different ratios of R_2/R_1, it is observed that although higher fragment collection

efficiencies seem to result from higher R_2/R_1 (see Fig. 2), the increased fuel-layer thickness required offsets this so that the overall efficiency suffers. For the chosen fixed parameters, the optimum efficiency is achieved at R_2/R_1 somewhere between 1.1 and 1.65.

Furthermore, the shape of the iso-efficiency curves, combined with the voltage breakdown curve, determines the optimum operating point, which, as seen in these cases, is significantly below 1 Mv. It is also shown that the optimum occurs at relatively small gap spacings, at which there is little difference between the two voltage breakdown curves.

To increase the efficiency significantly would require a reduction in temperature, the use of a more efficient moderator (probably also requiring a temperature reduction), or an increase in the overall reactor size.

The two-region concept does not seem to offer any advantage except at very low efficiencies. Therefore, this feature can probably be eliminated from further parametric studies.

APPENDIX A

Calculation of Minimum Fuel Thickness

For a given mass of fuel the minimum possible layer-thickness will result from the maximum cathode area:

$$S = 2\pi R_1 nH \, ,$$

where n is the number of cells and H is the reactor height. From the definition of the void fraction, it follows that

$$R_2^2 + R_0^2 - R_1^2 = \frac{\alpha V}{\pi nH} \, ,$$

where V is the reactor core volume. By eliminating nH from these two equations, S can be expressed as

$$S = \frac{2R_1 \alpha V}{R_2^2 + R_0^2 - R_1^2}$$

$$= \frac{2R_1 \alpha V}{(R_2 - R_1)^2 + \left(\dfrac{R_0}{R_1}\right)^2 R_1^2 + 2R_1(R_2 - R_1)} \, .$$

The latter expression is now used to maximize S with respect to R_1, holding both $(R_2 - R_1)$ and R_0/R_1 constant. This gives the relationship

$$R_1 = \frac{R_2 - R_1}{R_0/R_1} = \frac{d}{R_0/R_1} \, .$$

Thus the maximum value of S is

$$S = \frac{2\alpha V}{d\left(2 + \dfrac{d}{R_1}\right) + \dfrac{R_0^2}{R_1}} = \frac{2\alpha V}{d\left(1 + \dfrac{R_2}{R_1}\right) + \dfrac{R_0^2}{R_1}} \, .$$

The minimum fuel thickness is then

$$T = \frac{Xm'}{S} = \frac{Xm'}{\alpha V}\left[\frac{d(1 + R_2/R_1) + \dfrac{R_0^2}{R_1}}{2}\right] \, .$$

APPENDIX B

Tables of Overall Efficiencies

The following are tables of overall efficiencies for various values of P, R_2/R_1, d, α, and X.

Table B-1. Overall efficiency, $P = 0.5$, $R_2/R_1 = 1.1$

α	$X = 1$	$X = 0.8$	$X = 0.6$	$X = 0.4$
	$d = 0.24$			
.45	.0272	.0271	.0236	.0201
.40	.0302	.0281	.0248	—
.35	.0312	.0288	.0254	—
.25	.0306	.0283	.0248	—
	$d = 0.48$			
.45	.0170	.0200	.0183	.0168
.40	.0215	.0215	.0205	.0179
.35	.0230	.0227	.0214	.0174
.25	.0224	.0222	.0208	.0173
	$d = 0.71$			
.45	.0106	.0140	.0137	.0141
.40	.0146	.0162	.0167	.0157
.35	.0165	.0178	.0178	.0155
.25	.0155	.0171	.0170	.0154
	$d = 0.95$			
.45	.0071	.0101	.0100	.0118
.40	.0104	.0118	.0135	.0136
.35	.0117	.0133	.0149	.0137
.25	.0112	.0126	.0141	.0134

Table B-2. Overall efficiency, $P = 0.75$, $R_2/R_1 = 1.1$

α	$X = 1$	$X = 0.8$	$X = 0.6$	$X = 0.4$
	$d = 0.24$			
.45	.0343	.0346	.0302	.0253
.40	.0385	.0361	.0317	—
.35	.0397	.0370	.0323	—
.25	.0392	.0364	.0317	—
	$d = 0.48$			
.45	.0212	.0249	.0230	.0214
.40	.0268	.0271	.0261	.0230
.35	.0288	.0288	.0272	.0222
.25	.0279	.0279	.0264	.0222
	$d = 0.71$			
.45	.0145	.0177	.0171	.0177
.40	.0186	.0201	.0210	.0199
.35	.0206	.0221	.0223	.0197
.25	.0196	.0210	.0214	.0195
	$d = 0.95$			
.45	.0107	.0136	.0130	.0146
.40	.0142	.0153	.0167	.0172
.35	.0157	.0170	.0183	.0174
.25	.0150	.0160	.0174	.0170

Table B-3. Overall efficiency, $P = 1.3$, $R_2/R_1 = 1.1$

α	$X = 1$	$X = 0.8$	$X = 0.6$	$X = 0.4$
	$d = 0.24$			
.45	.0405	.0424	.0376	.0325
.40	.0467	.0445	.0402	—
.35	.0487	.0460	.0413	—
.25	.0477	.0452	.0404	—
	$d = 0.48$			
.45	.0232	.0281	.0265	.0258
.40	.0297	.0312	.0311	.0285
.35	.0327	.0336	.0326	.0277
.25	.0314	.0324	.0315	.1276
	$d = 0.71$			
.45	.0158	.0193	.0189	.0204
.40	.0204	.0222	.0237	.0237
.35	.0225	.0244	.0257	.0237
.25	.0215	.0232	.0241	.0234
	$d = 0.95$			
.45	.0114	.0149	.0143	.0161
.40	.0155	.0169	.0185	.0197
.35	.0173	.0185	.0202	.0202
.25	.0166	.0177	.0191	.0197

Table B-4. Overall efficiency, $P = 0.5$, $R_2/R_1 = 1.65$

α	$X = 1$	$X = 0.8$	$X = 0.6$	$X = 0.4$	$X = 0.2$	$X = 0.1$
	$d = 0.19$					
.45	.0305	.0311	.0274	—	—	—
.40	.0344	.0326	.0297	—	—	—
.35	.0356	.0337	.0307	—	—	—
.25	.0350	.0331	.0298	—	—	—
	$d = 0.38$					
.45	.0192	.0219	.0202	—	—	—
.40	.0237	.0240	.0232	—	—	—
.35	.0255	.0253	.0243	—	—	—
.25	.0247	.0247	.0235	—	—	—
	$d = 0.75$					
.45	.0100	.0126	.0119	.0129	.0119	—
.40	.0135	.0140	.0149	.0151	.0122	—
.35	.0145	.0153	.0162	.0153	.0123	—
.25	.0140	.0147	.0155	.0150	.0112	—
	$d = 1.13$					
.45	—	.0083	.0084	.0092	.0097	.0072
.40	.0070	.0100	.0105	.0114	.0104	.0073
.35	.0092	.0111	.0115	.0118	.0106	.0071
.25	.0090	.0105	.0108	.0114	.0096	.0066

Table B-5. Overall efficiency, $P = 1.0$, $R_2/R_1 = 1.65$

α	$X = 1$	$X = 0.8$	$X = 0.6$	$X = 0.4$	$X = 0.2$	$X = 0.1$
	$d = 0.19$					
.45	.0495	.0522	.0465	—	—	—
.40	.0575	.0554	.0503	—	—	—
.35	.0602	.0577	.0516	—	—	—
.25	.0587	.0565	.0503	—	—	—
	$d = 0.38$					
.45	.0290	.0344	.0318	—	—	—
.40	.0370	.0376	.0378	—	—	—
.35	.0400	.0405	.0401	—	—	—
.25	.0386	.0390	.0387	—	—	—
	$d = 0.25$					
.45	.0145	.0183	.0176	.0201	.0197	—
.40	.0192	.0208	.0231	.0238	.0207	—
.35	.0213	.0230	.0253	.0244	.0209	—
.25	.0203	.0218	.0240	.0237	.0191	—
	$d = 1.13$					
.45	—	.0122	.0119	.0135	.0153	.0123
.40	.0128	.0140	.0154	.0176	.0171	.0123
.35	.0140	.0156	.0170	.0184	.0175	.0120
.25	.0135	.0148	.0162	.0178	.0159	.0112

Table B-6. Overall efficiency, $P = 1.5$, $R_2/R_1 = 1.65$

α	$X = 1$	$X = 0.8$	$X = 0.6$	$X = 0.4$	$X = 0.2$	$X = 0.1$
	$d = 0.19$					
.45	.0555	.0596	.0537	—	—	—
.40	.0652	.0638	.0584	—	—	—
.35	.0690	.0668	.0598	—	—	—
.25	.0670	.0651	.0586	—	—	—
	$d = 0.38$					
.45	.0318	.0372	.0351	.0359	—	—
.40	.0398	.0416	.0426	.0407	—	—
.35	.0433	.0450	.0455	.0401	—	—
.25	.0418	.0432	.0437	.0396	—	—
	$d = 0.75$					
.45	.0152	.0193	.0185	.0215	.0225	—
.40	.0202	.0220	.0244	.0263	.0239	—
.35	.0225	.0242	.0271	.0271	.0242	—
.25	.0214	.0230	.0255	.0263	.0220	—
	$d = 1.13$					
.45	—	.0125	.0124	.0143	.0168	.0142
.40	.0120	.0146	.0163	.0186	.0193	.0143
.35	.0148	.0163	.0180	.0196	.0200	.0139
.25	.0140	.0154	.0170	.0189	.0179	.0130

Table B-7. Overall efficiency, $P = 0.75$, $R_2/R_1 = 1.65$

α	X = 1	X = 0.8	X = 0.6	X = 0.4	X = 0.2	X = 0.1
			$d = 0.19$			
.45	.0407	.0424	.0378	—	—	—
.40	.0468	.0449	.0411	—	—	—
.35	.0490	.0468	.0424	—	—	—
.25	.0480	.0458	.0416	—	—	—
			$d = 0.38$			
.45	.0252	.0292	.0270	—	—	—
.40	.0317	.0320	.0310	—	—	—
.35	.0340	.0339	.0327	—	—	—
.25	.0330	.0328	.0316	—	—	—
			$d = 0.75$			
.45	.0130	.0165	.0157	.0172	.0161	—
.40	.0174	.0187	.0198	.0203	.0168	—
.35	.0192	.0202	.0217	.0204	.0170	—
.25	.0184	.0194	.0204	.0200	.0155	—
			$d = 1.13$			
.45	—	.0108	.0106	.0121	.0130	.0100
.40	.0115	.0126	.0140	.0151	.0140	.0100
.35	.0126	.0140	.0153	.0158	.0143	.0099
.25	.0120	.0133	.0145	.0151	.0130	.0092

Table B-8. Overall efficiency, $P = 0.5$, $R_2/R_1 = 2.72$

α	X = 1	X = 0.8	X = 0.6	X = 0.4	X = 0.2	X = 0.1
			$d = 0.27$			
.45	.0188	.0208	.0190	.0190	—	—
.40	.0225	.0225	.0224	.0212	—	—
.35	.0240	.0238	.0240	.0208	—	—
.25	.0233	.0232	.0230	.0207	—	—
			$d = 0.54$			
.45	.0102	.0132	.0123	.0123	.0119	—
.40	.0142	.0146	.0145	.0142	.0126	—
.35	.0154	.0156	.0154	.0141	.0125	—
.25	.0149	.0150	.0148	.0138	.0115	—
			$d = 0.81$			
.45	—	.0081	.0087	.0095	.0087	—
.40	—	.0102	.0112	.0110	.0101	—
.35	.0098	.0115	.0119	.0112	.0105	—
.25	.0090	.0110	.0115	.0109	.0094	—
			$d = 1.08$			
.45	—	—	—	.0077	.0076	.0065
.40	—	—	.0086	.0093	.0084	.0068
.35	—	.0076	.0096	.0093	.0086	.0067
.25	—	—	.0090	.0091	.0078	.0062

Table B-9. Overall efficiency, $P = 1.5$, $R_2/R_1 = 2.72$

α	X = 1	X = 0.8	X = 0.6	X = 0.4	X = 0.2	X = 0.1
			$d = 0.27$			
.45	.0343	.0414	.0388	.0401	—	—
.40	.0442	.0459	.0471	.0454	—	—
.35	.0480	.0499	.0508	.0446	—	—
.25	.0462	.0472	.0484	.0441	—	—
			$d = 0.54$			
.45	.0177	.0216	.0206	.0240	.0249	—
.40	.0231	.0244	.0273	.0290	.0267	—
.35	.0250	.0271	.0302	.0294	.0272	—
.25	.0242	.0255	.0285	.0285	.0248	—
			$d = 0.81$			
.45	—	.0145	.0145	.0159	.0186	—
.40	—	.0172	.0182	.0207	.0213	—
.35	.0171	.0190	.0197	.0218	.0221	—
.25	.0160	.0181	.0189	.0210	.0198	—
			$d = 1.08$			
.45	—	—	—	.0125	.0149	.0138
.40	—	—	.0142	.0154	.0171	.0145
.35	—	.0138	.0157	.0163	.0181	.0145
.25	—	—	.0149	.0156	.0162	.0134

Table B-10. Overall efficiency, $P = 0.75$, $R_2/R_1 = 2.72$

α	X = 1	X = 0.8	X = 0.6	X = 0.4	X = 0.2	X = 0.1
			$d = 0.27$			
.45	.0258	.0291	.0264	.0259	—	—
.40	.0316	.0312	.0301	.0294	—	—
.35	.0337	.0329	.0326	.0291	—	—
.25	.0328	.0322	.0310	.0288	—	—
			$d = 0.54$			
.45	.0133	.0166	.0158	.0173	.0161	—
.40	.0179	.0186	.0202	.0198	.0173	—
.35	.0193	.0206	.0219	.0195	.0175	—
.25	.0187	.0196	.0209	.0192	.0160	—
			$d = 0.81$			
.45	—	.0108	.0111	.0122	.0126	—
.40	—	.0131	.0140	.0154	.0136	—
.35	.0129	.0147	.0151	.0159	.0143	—
.25	.0120	.0140	.0143	.0154	.0127	—
			$d = 1.08$			
.45	—	—	—	.0097	.0108	.0089
.40	—	—	.0109	.0118	.0117	.0094
.35	—	.0101	.0122	.0124	.0119	.0093
.25	—	—	.0115	.0119	.0108	.0086

Table B-11. Overall efficiency, $P = 1.0$, $R_2/R_1 = 2.72$

α	$X = 1$	$X = 0.8$	$X = 0.6$	$X = 0.4$	$X = 0.2$	$X = 0.1$
			$d = 0.27$			
.45	.0308	.0360	.0323	.0323	—	—
.40	.0390	.0391	.0383	.0367	—	—
.35	.0418	.0415	.0410	.0363	—	—
.25	.0403	.0403	.0394	.0359	—	—
			$d = 0.54$			
.45	.0156	.0193	.0185	.0212	.0202	—
.40	.0203	.0219	.0245	.0248	.0216	—
.35	.0226	.0244	.0267	.0246	.0219	—
.25	.0215	.0229	.0255	.0242	.0200	—
			$d = 0.81$			
.45	—	.0129	.0129	.0144	.0158	—
.40	—	.0153	.0164	.0186	.0173	—
.35	.0151	.0168	.0177	.0194	.0179	—
.25	.0141	.0160	.0171	.0187	.0159	—
			$d = 1.08$			
.45	—	—	—	.0111	.0132	.0111
.40	—	—	.0127	.0139	.0146	.0117
.35	—	.0121	.0140	.0147	.0150	.0117
.25	—	—	.0132	.0141	.0136	.0108

NOMENCLATURE

σ_f microscopic fission cross section

$\sum_a^M$ macroscopic absorption cross section, excluding fuel

$\sum_a^F$ macroscopic absorption cross section of fuel

τ neutron age to thermal

L^M diffusion length of thermal neutrons excluding fuel

L diffusion length of thermal neutrons including fuel

M^2 migration area

ν average number of neutrons emitted per fission

η average number of neutrons emitted per absorption in fuel

B^2 buckling of reactor (Laplacian)

k_∞ infinite criticality factor

$\mathcal{M}$ multiplication factor

m critical mass of fuel

m' total fuel loading

A atomic weight of fuel

N_0 Avogadro's number

V total reactor volume

α ratio of void volume to total volume

$\mathcal{E}$ efficiency

E^0 initial fission-fragment energy

Z^0 initial fission-fragment charge number

e initial fission-fragment charge

P fission cell potential

T fuel-layer thickness

R_0 coolant channel radius

R_1 cathode radius

R_2 anode radius

S fuel-layer area

REFERENCES

1. Safonov, G., *The Fission–Electric Cell Project*, RM-3908-PR, RAND Corporation, Santa Monica, California, 1963.

2. Heindl, C. J., *Efficiency of Fission Electric Cells*, TR 32-105, Jet Propulsion Laboratory, Pasadena, California, May 25, 1961.

3. Shapiro, J. L., *The Two-Region Fission–Electric Cell Reactor*, TR 32-685, Jet Propulsion Laboratory, Pasadena, California, February 15, 1965.

4. Meghreblian, R. V., and Holmes, D. K., *Reactor Analysis*, McGraw-Hill Co., New York, 1960.

5. Weinberg, A. M., and Wigner, E. P., *The Physical Theory of Neutron Chain Reactors*, University of Chicago Press, 1958.

6. *Reactor Physics Constants*, ANL-5800, 2nd ed, United States Atomic Energy Commission, July 1963.

7. Behrens, D. J., "The Effect of Holes in a Reacting Material on the Passage of Neutrons," *Proceedings of the Physical Society (London)* Vol. 62A, pp. 607–616, 1949.

8. Alpert, D., and Lee, D., *Electrical Breakdown in High Vacuum*, Report R-129, Coordinated Science Laboratory, University of Illinois, 1962.